Electronic Supplementary Information

Supramolecular Helical Nanostructures from Self-Assembly of Coil-Rod-Coil Amphiphilic Molecules Incorporating Dianthranide Unit

Shengsheng Yu, Rui Sun, Tie Chen, Long Yi Jin*

Key Laboratory for Organism Resources of the Changbai Mountain and Functional Molecules, and Department of Chemistry,College of Science, Yanbian University, No. 977 Gongyuan Road, Yanji 133002, People's Republic of China.

*Corresponding author. E-mail address: lyjin@ybu.edu.cn.

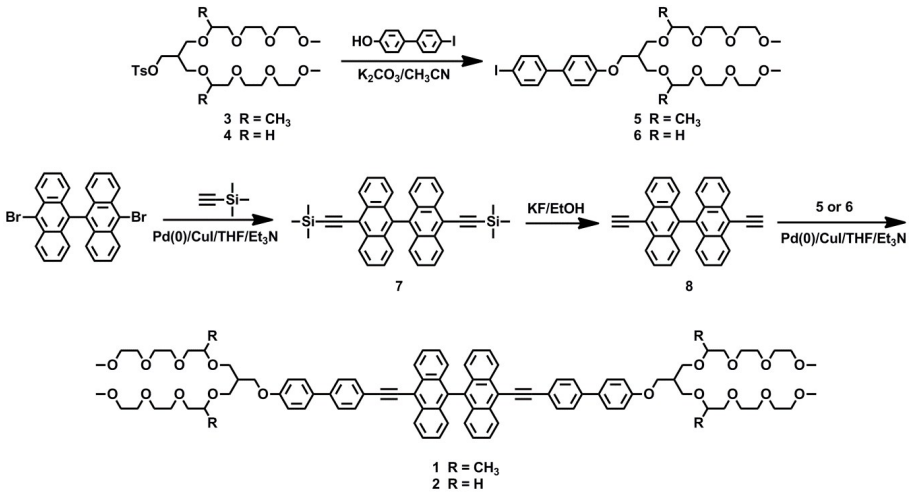

Scheme S1. Synthetic route of coil-rod-coil molecules **1** and **2**.

Experimental

Diethylene glycol methyl ether, triethylene glycol monomethyl ether, lithium aluminum hydride, L-Lactic acid ethyl ester, toluene-p-sulfonyl chloride (TsCl, 99%), pyridine, Trimethylsilyl-acetylene, CuI, tetrakis(triphenylphosphine) palladium (0), 10,10'-dibromo-9,9'-bianthracene, potassium carbonate, triethylamine (99.5%), 4-Hydroxy-4'-iodobiphenyl, potassium fluoride, 2,3,5,6-Tetrafluoro-7,7,8,8-tetracyanoquinodimethane (4F-TCNQ) and conventional reagents were used as received.

Synthesis of compounds 3 and 4.

Compounds **3** and **4** were prepared according to the similar procedures described elsewhere [S1, S2].

Synthesis 5 and 6. These compounds were synthesized according to the same procedure, a representation example is described for **6**. 4-Hydroxy-4'-iodobiphenyl (0.385 g, 1.30 mmol), compound **3** (0.6 g, 1mmol) and excess K_2CO_3 (0.599 g, 4.30 mmol) were dissolved in 55 ml acetonitrile. The mixture was refluxed for 24 h. The resulting solution was poured into water and extracted with methylene chloride and ethyl acetate, dried over anhydrous magnesium sulfate, and filtered. The solvent was

removed in a rotary evaporator, and the crude product was purified by column chromatography (silica gel) using methylene chloride: ethyl acetate (10:1 v/v) as eluent to yield 0.50 g (68.4 %).

Compound 5: ^{1}H-NMR (300 MHz, $CDCl_3$, δ, ppm) 7.72 (d, *J* = 4 Hz，2H), 7.46 (d, *J* = 4 Hz，2H), 7.28 (d, *J* = 4Hz, 2H), 6.97 (d, *J* = 4 Hz，2H), 4.07 (d, *J* = 3 Hz，2H), 3.46-3.69 (m, 26H), 3.36 (s, 6H), 2.27-2.40 (m, 1H), 1.12-1.15 (m, 6H).

Compound 6: ^{1}H-NMR (300 MHz, $CDCl_3$, δ, ppm) 7.72 (d, *J* = 4 Hz，2H), 7.46 (d, *J* = 4 Hz, 2H), 7.28 (d, *J* = 4 Hz, 2H), 6.97 (d, *J* = 4 Hz，2H), 4.08 (d, *J* = 3 Hz, 2H), 3.51-3.69 (m, 28H), 3.36 (s, 6H), 2.39-2.46 (m, 1H).

Synthesis of 7. 10,10'-Dibromo-9,9'-bianthracene (1.0 g, 1.9 mmol) and trimethylsilyl-acetylene (0.265 g, 9.72 mmol) were dissolved in 25 ml of tetrahydrofuran and 20 ml of triethylamine and degassed. CuI (36.17 mg, 0.19 mmol) and tetrakis(triphenylphosphine) palladium (0) (219.55 mg, 0.19 mmol) were added to the solution. The mixture was heated at reflux for 24 h under nitrogen and kept away from the light. The resulting solution was poured into water and extracted with methylene chloride and ethyl acetate, dried over anhydrous magnesium sulfate, and filtered. The solvent was removed in a rotary evaporator, and the crude product was purified by column chromatography (silica gel) using petroleum ether as eluent to yield 0.54 g (50.7 %).

^{1}H-NMR (300 MHz, $CDCl_3$, δ, ppm) 8.78 (s, 4H), 7.55 (s, 4H), 7.16 (s, 4H), 7.05 (s, 4H), 0.48 (s, 18H).

Synthesis of 8. Compound 7 (0.54 g, 0.98 mmol) and potassium fluoride (0.57 g, 9.8 mmol) were dissolved in 60 ml ethyl alcohol. The mixture was refluxed for 12 h. The resulting solution was poured into water and extracted with methylene chloride and ethyl acetate, dried over anhydrous magnesium sulfate, and filtered. The solvent was removed in a rotary evaporator, and the crude product was purified by column chromatography (silica gel) using petroleum ether as eluent to yield 0.30 g (76.3 %).

^{1}H-NMR (300 MHz, $CDCl_3$, δ, ppm) 8.75 (s, 4H), 7.57 (s, 4H), 7.19 (s, 4H), 7.09 (s, 4H), 4.13 (s, 2H).

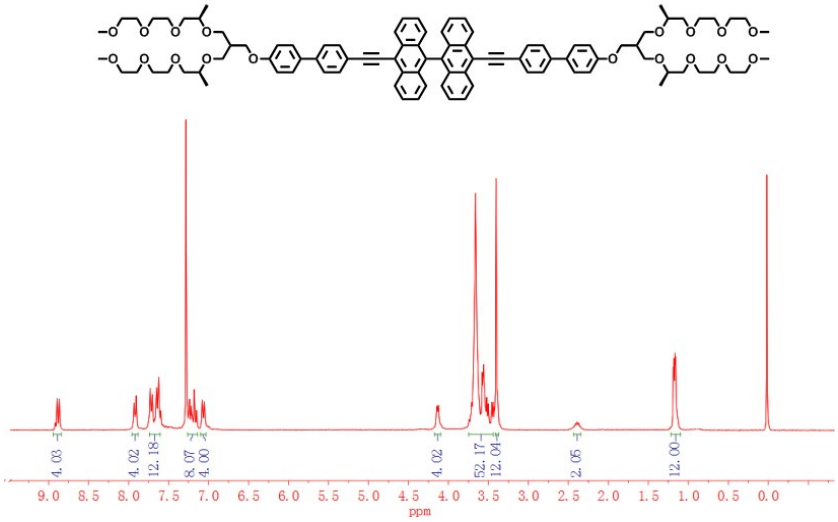

Fig. S1 ^{1}H-NMR spectrum of molecule **1**.

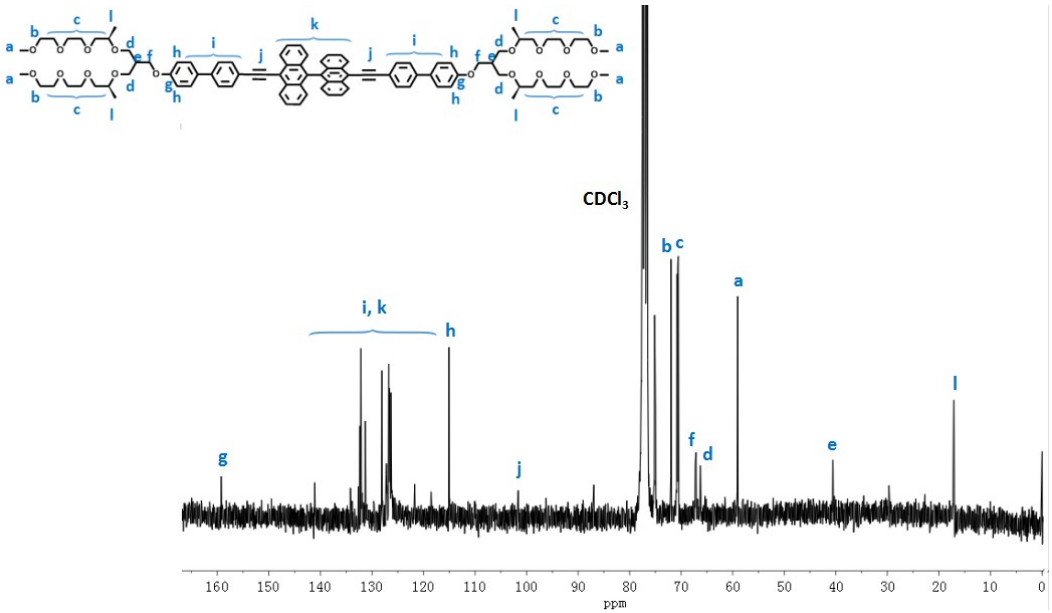

Fig. S2 ^{13}C-NMR spectrum of molecule **1**.

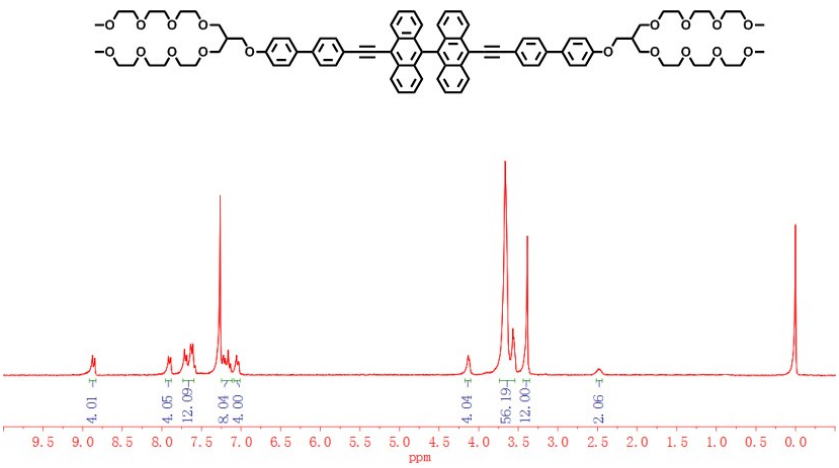

Fig. S3 ^{1}H-NMR spectrum of molecule **2**.

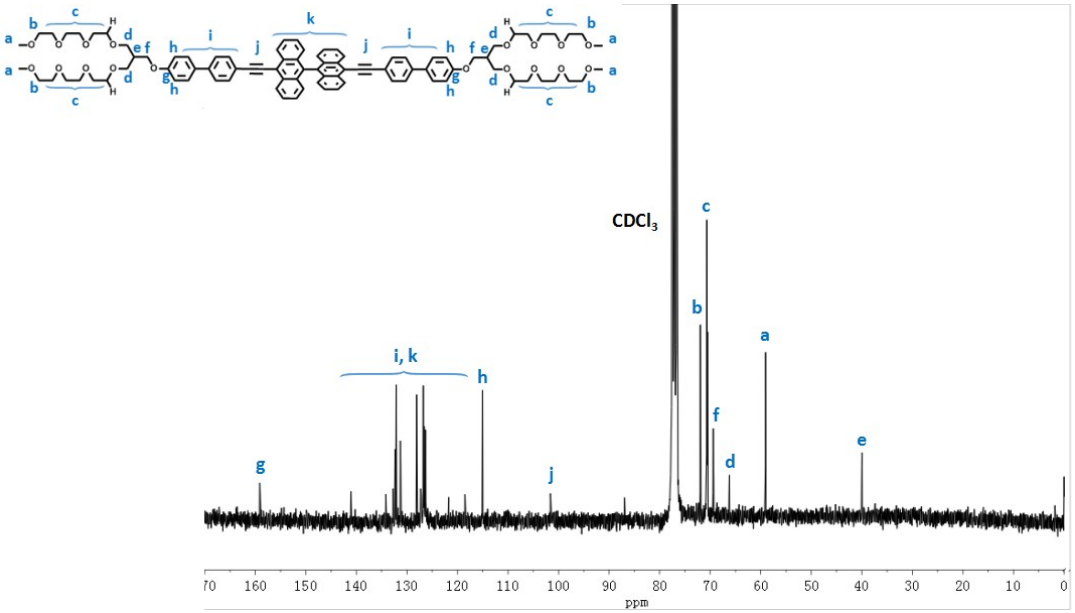

Fig. S4 ^{13}C-NMR spectrum of molecule **2**.

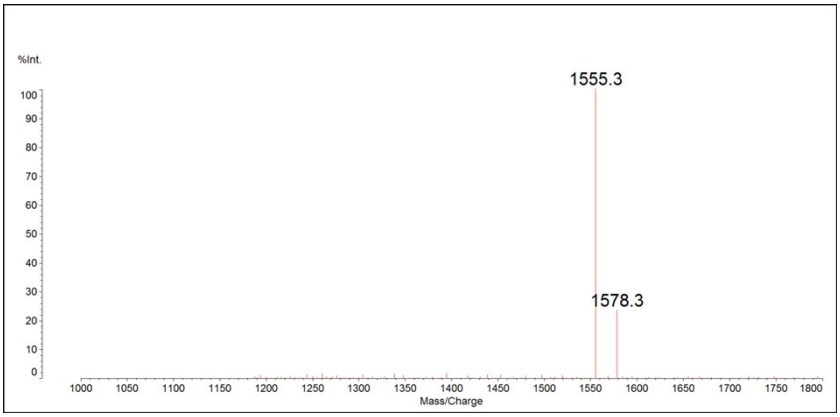

Fig. S5 MALDI-TOF mass spectrum of molecule **1**.

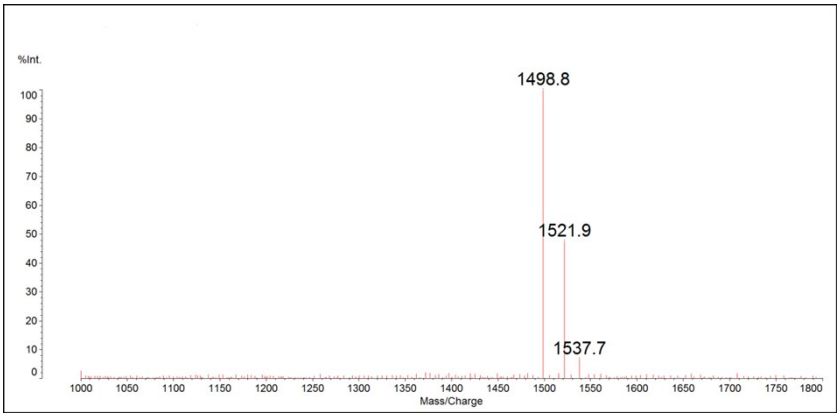

Fig. S6 MALDI-TOF mass spectrum of molecule **2**.

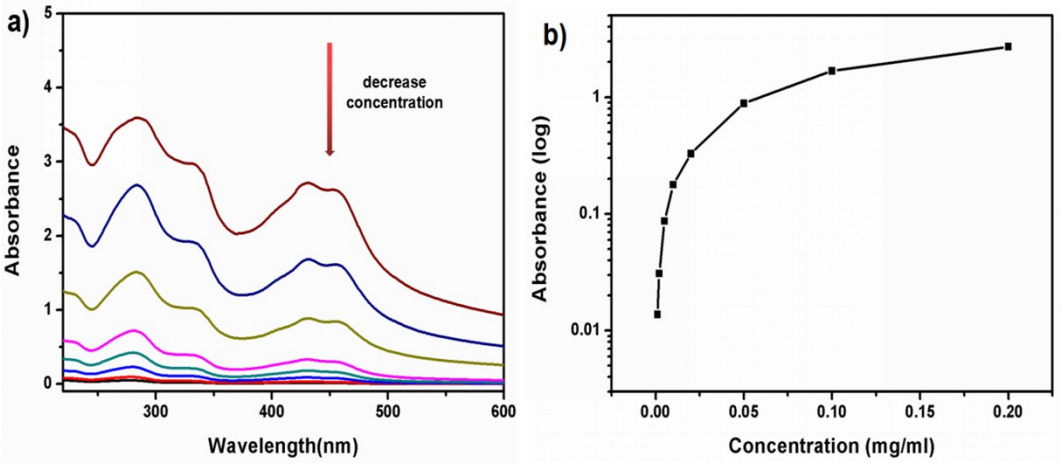

Fig. S7 a) Concentration dependent UV-Vis spectra of molecule **1** (from up to down 0.2, 0.1, 0.05, 0.02, 0.01, 0.005, 0.002 and 0.001 mg/ml, respectively) and b) the curve between the absorbance versus molecular concentration of **1** in aqueous solution (at 430 nm).

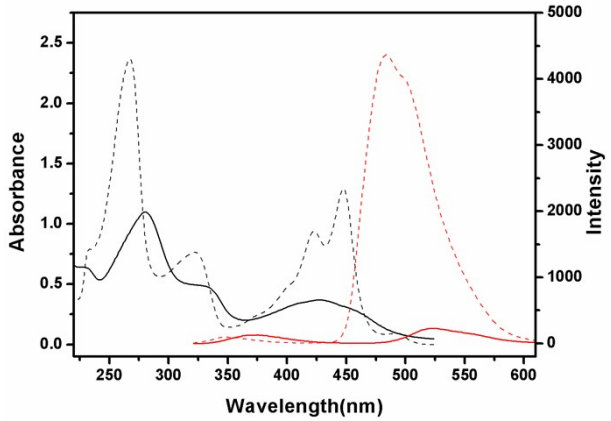

Fig. S8 Absorption (black) and emission spectra (red) of **2** in THF (dash) and in aqueous solution (solid) with 0.002 wt %. (Fluorescence slit width: Ex bandwidth: 5 nm; Em bandwidth: 5 nm).

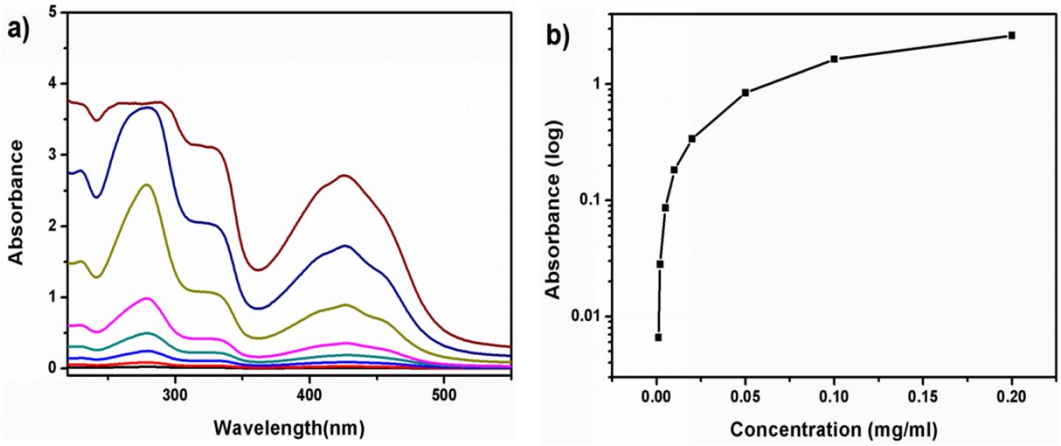

Fig. S9 a) Concentration dependent UV-Vis spectra of molecule **2** (from up to down 0.2, 0.1, 0.05, 0.02, 0.01, 0.005, 0.002 and 0.001 mg/ml, respectively) and b) the curve between the absorbance versus molecular concentration of **2** in aqueous solution (at 434 nm).

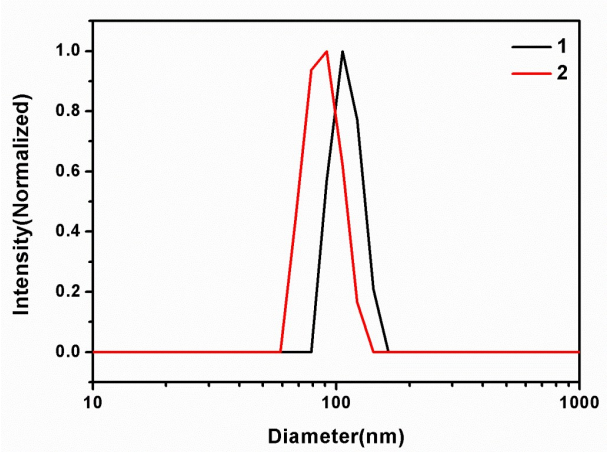

Fig. S10 Size distribution graphs of **1** and **2** in aqueous solution (0.01 wt %).

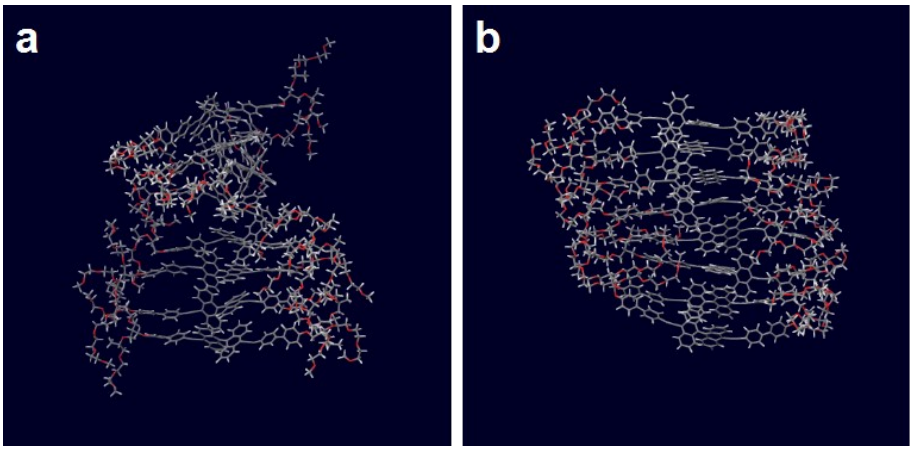

Fig. S11 Molecular dynamic simulation results of (a) **1**, (b) **2** in water environment.

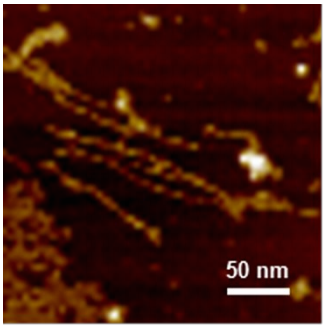

Fig. S12 AFM image of molecule **1** in diluted aqueous solution.

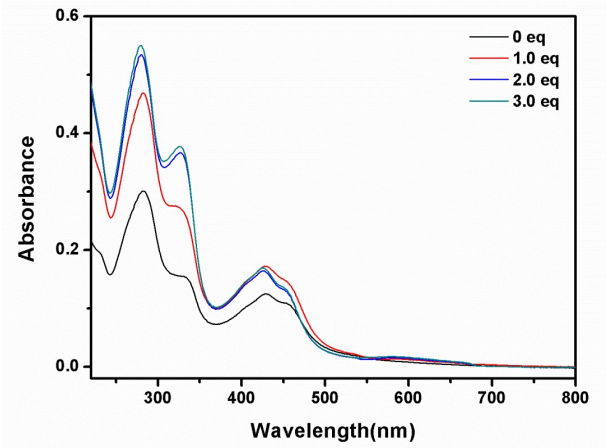

Fig. S13 Absorption spectra of **1** upon the addition of 4F-TCNQ in aqueous solution (0.001 wt %)

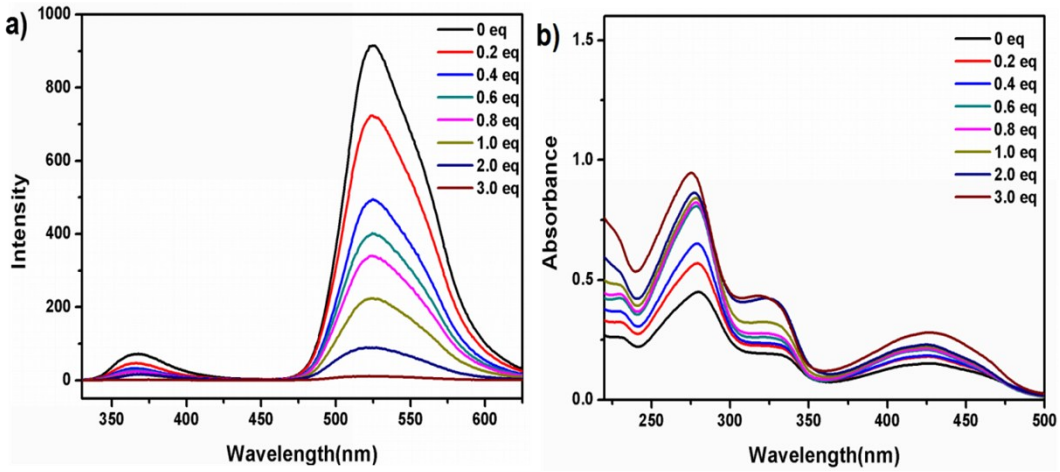

Fig. S14 (a) Fluorescence and (b) absorption spectra of **2** upon the addition of 4F-TCNQ in aqueous solution (0.001 wt %). (Fluorescence slit width: Ex bandwidth: 5 nm; Em bandwidth: 5 nm).

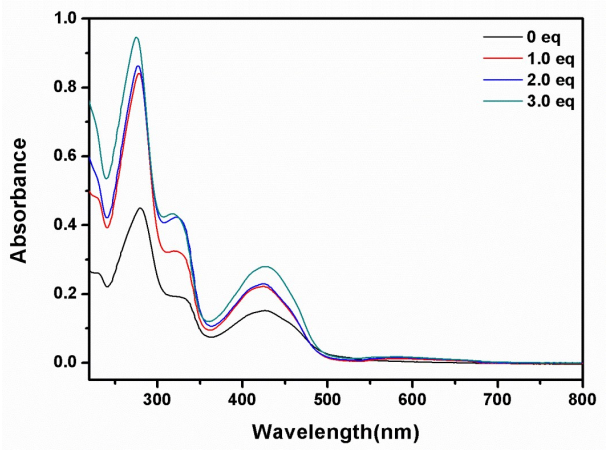

Fig. S15 Absorption spectra of **2** upon the addition of 4F-TCNQ in aqueous solution (0.001 wt %).

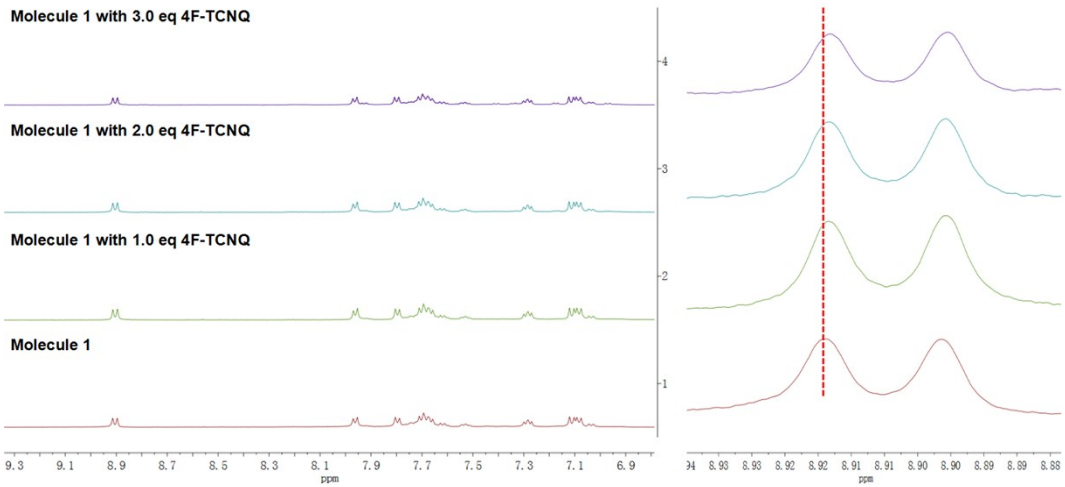

Fig. S16 ^{1}H-NMR experiments of molecule **1** with various concentrations of 4F-TCNQ in CD_3CN.

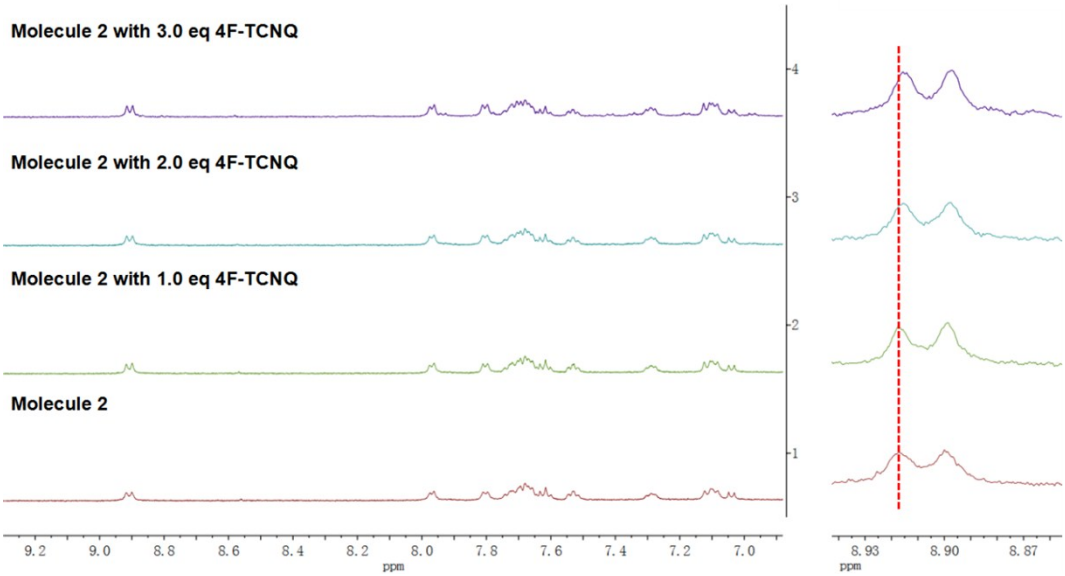

Fig. S17 ^{1}H-NMR experiments of molecule **2** with various concentrations of 4F-TCNQ in CD_3CN.

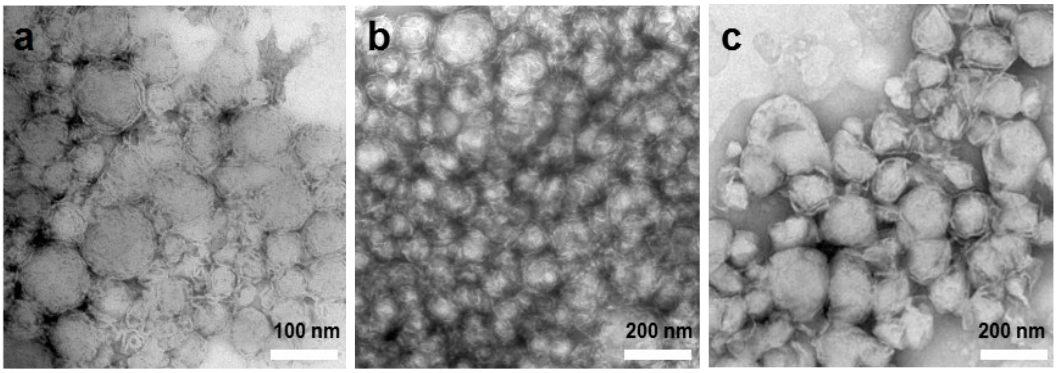

Fig. S18 Negative-staining TEM images of **1** with (a) 0 equiv., (b) 0.6 equiv. and (c) 1.0 equiv. 4F-TCNQ (all samples cast from 0.01 wt % aqueous solutions and negatively stained with uranyl acetate).

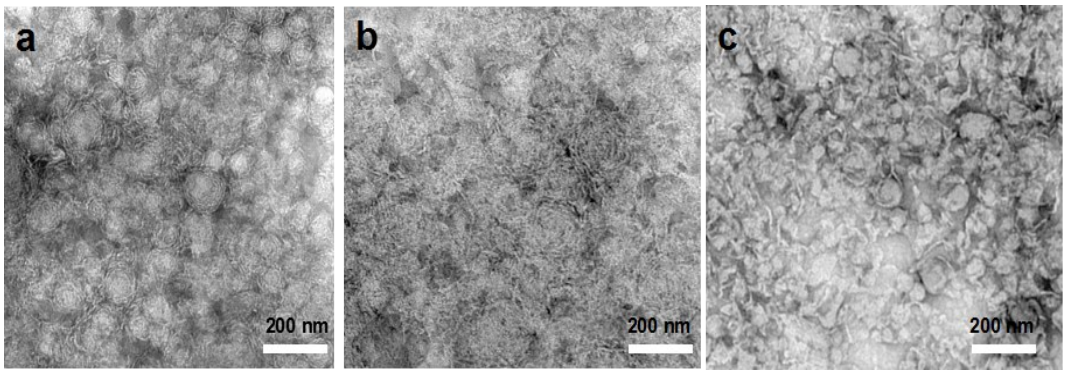

Fig. S19 Negative-staining TEM images of **2** with (a) 0 equiv., (b) 0.6 equiv. and (c) 1.0 equiv. 4F-TCNQ (all samples cast from 0.01 wt % aqueous solutions and negatively stained with uranyl acetate).

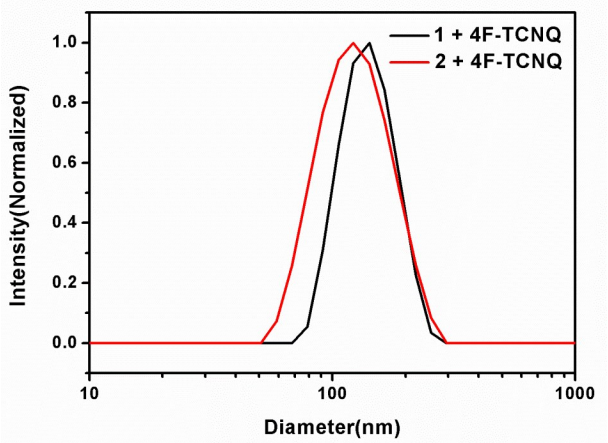

Fig. S20 Size distribution graphs of **1** and **2** with 1.0 equiv. 4F-TCNQ in aqueous solution (0.01 wt %).

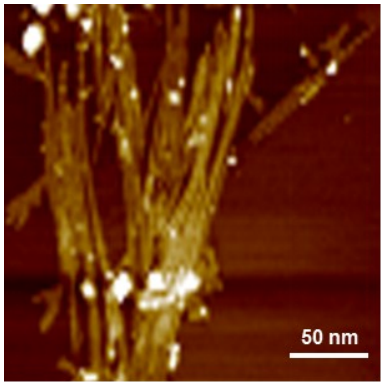

Fig. S21 AFM image of molecule **1** with 1.0 equiv. 4F-TCNQ in aqueous solution (0.01 wt %).

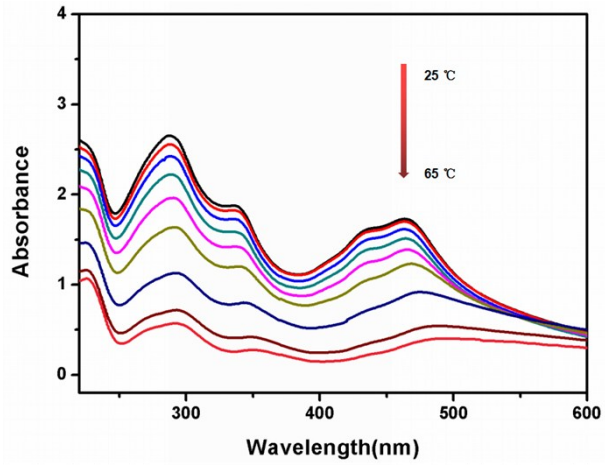

Fig. S22 Temperature-dependent absorption spectra of **1** in aqueous solution (0.01 wt %).

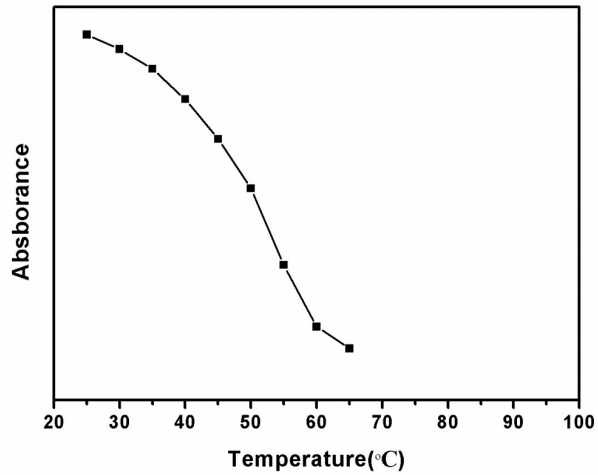

Fig. S23 The curve between the absorbance versus temperature of molecule **1** in aqueous solution (at 287 nm).

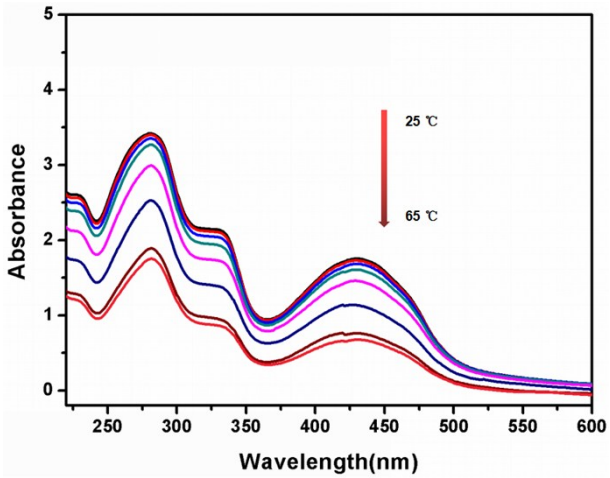

Fig. S24 Temperature-dependent absorption spectra of **2** in aqueous solution (0.01 wt %).

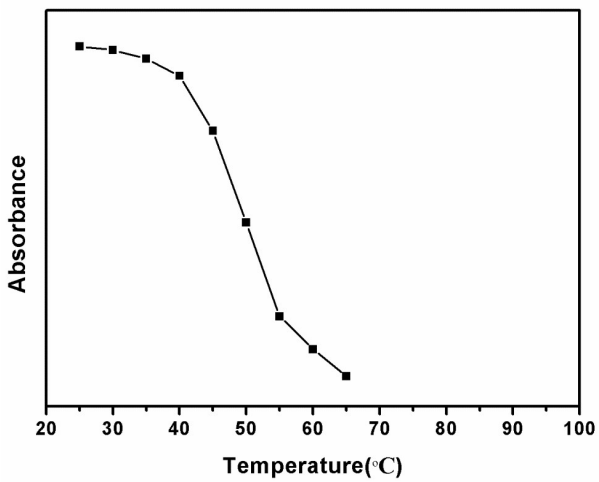

Fig. S25 The curve between the absorbance versus temperature of molecule **2** in aqueous solution (at 281 nm).

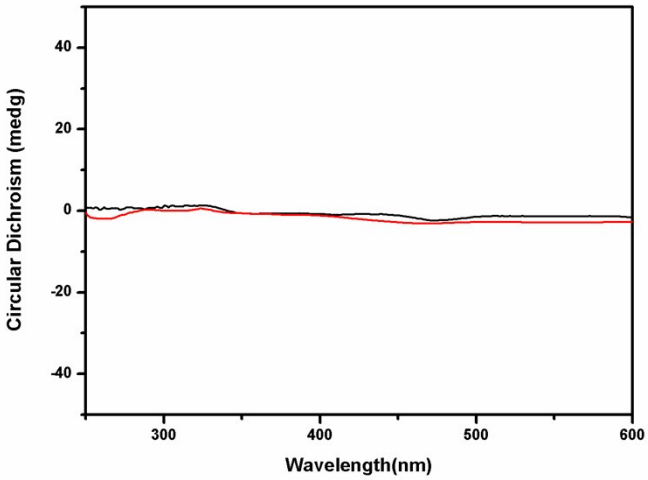

Fig. S26 CD spectra of molecule 2 (black) and molecule 2 with 1.0 equiv. of 4F-TCNQ (red) in aqueous solution (0.01 wt %).

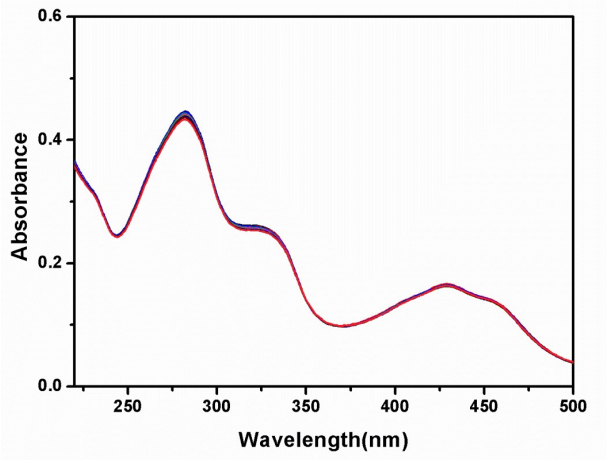

Fig. S27 Temperature-dependent absorption spectra (25-65 ℃) of **1** upon the addition of 1.0 equiv. 4F-TCNQ in aqueous solution (0.001 wt %).

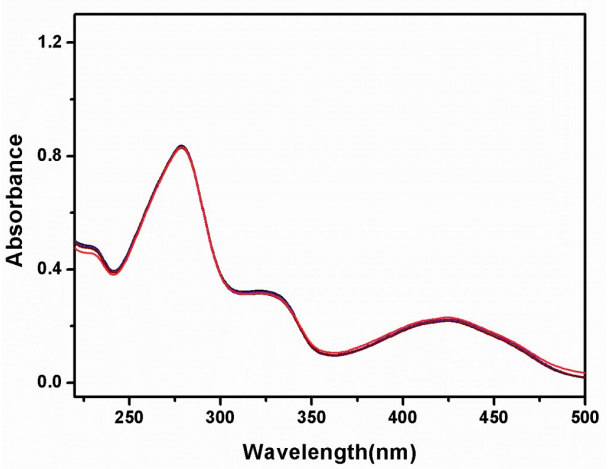

Fig. S28 Temperature-dependent absorption spectra (25-65 ℃) of **2** upon the addition of 1.0 equiv. 4F-TCNQ in aqueous solution (0.001 wt %).

References

[S1] D.-J. Hong, E. Lee, M.-G. Choi, M. Lee, Self-organized spiral columns in laterally grafted rods. *Chem. Commun.,* 2010, **46,** 4896-4898.

[S2] Y. Kim, S. Shin, T. Kim, D. Lee, C. Seok, M. Lee, Switchable nanoporous sheets by the aqueous self-assembly of aromatic macrobicycles. *Angew. Chem. Int. Ed.,* 2013, **52,** 6424-6428.